

Cite this: *Nanoscale*, 2014, 6, 14508

# A gate controlled molecular switch based on picene–F<sub>4</sub>TCNQ charge-transfer material†

Torsten Hahn,\* Simon Liebing and Jens Kortus

We show that the recently synthesized charge-transfer material picene–F<sub>4</sub>TCNQ can be used as a gate-voltage controlled molecular switch. The picene–F<sub>4</sub>TCNQ system is compared with the extensively characterized anthraquinone-based molecular system, which is known to exhibit large switching ratios due to quantum interference effects. In the case of picene–F<sub>4</sub>TCNQ we find switching ratios larger by one order of magnitude. Further, our calculations reveal that the picene–F<sub>4</sub>TCNQ system resembles remarkably well the *I*–*V* characteristics of a classical diode. The reverse-bias current of this molecular diode can be increased two orders of magnitude by an external gate voltage. Based on density-functional theory calculations we show that the hybrid states formed by the picene–F<sub>4</sub>TCNQ system play the key role in determining transport properties. We further conclude that the tuning of quantum transport properties through hybrid states is a general concept which opens a new route towards functional materials for molecular electronics.

Received 6th May 2014,  
Accepted 23rd September 2014

DOI: 10.1039/c4nr02455a

www.rsc.org/nanoscale

## 1. Introduction

The basic idea underlying molecular electronics is that the typical functionality needed to build integrated circuits has to be realized by single molecules. This idea was already part of the pioneering theoretical description of a molecular diode given by Ratner and coworkers many years ago.<sup>1</sup> Since then, why it is not easy to actually build a satisfying molecular version of the classical semiconductor diode has been repeatedly discussed.<sup>2–4</sup> In practice we face the problem of the *I*–*V* characteristics being rather symmetrical in nearly all molecular devices even when using a highly asymmetric molecule. As a result the attempts to manufacture molecular diodes or transistors resulted in rather poor rectification or switching ratios compared to conventional semiconductor devices.<sup>5</sup> The criteria for achieving diode-like high rectification ratios in molecular junctions have already been suggested by Ratner *et al.*<sup>1</sup> Their proposal was that organic charge-transfer materials where two molecular subunits each carry an opposite charge should be suitable for the task. However, from this theoretical work it was also concluded that a strong coupling between the molecular subunits may completely screen the desired effect.

Recently this idea was picked up by Tsuji *et al.*,<sup>6</sup> and they presented rectification ratios  $R = 2 \cdots 3$ . In this paper we present

theoretical results on the charge transfer material picene–F<sub>4</sub>TCNQ.<sup>7</sup> This material was synthesized very recently for the first time and the experiments indicated new electronic states due to the charge transfer. These electronic levels close to the Fermi energy are beneficial for transport, and the additional flat geometry together with the weak  $\pi$ – $\pi$  coupling of the molecular building blocks is a perfect match for the requirements given by Ratner.

We show that this system can reach much higher rectification ratios up to  $R \approx 20$ , which is at least one order of magnitude higher than other values reported previously. Our system also exceeds the recently published results by Batra and coworkers in terms of achievable values for  $R$ .<sup>11</sup> We compare our theoretical results to calculations on an anthraquinone based molecular switch. The anthraquinone system was chosen because it is well characterized and known to perform as a molecular switch.<sup>8–10</sup> Furthermore, theoretical calculations with different contact materials and reliable measurements are available for comparison with our results.<sup>12–15</sup> We also investigate the dependence of the *I*–*V* characteristics on an external gate voltage. Apart from electrochemical gating<sup>16</sup> or redox active switching<sup>12</sup> this seems to be the most promising way to manufacture working active electronic devices.

## 2. Results and discussion

The material under consideration here is built from picene and fluorinated TCNQ molecules forming molecular crystals or films with an 1 : 1 composition which can be synthesized by

TU Freiberg, Institute of Theoretical Physics, Leipziger Str. 23, D-09596 Freiberg, Germany. E-mail: torsten.hahn@physik.tu-freiberg.de; Fax: +49 (0)3731 394005; Tel: +49 (0)3731 394034

†Electronic supplementary information (ESI) available. See DOI: 10.1039/C4NR02455A

co-evaporation.<sup>7</sup> The main building block in the crystal is a dimer like structure of picene and TCNQ with flat orientation with respect to each other. Therefore, we start our discussion with a short comparison of the electronic structure of the free

picene-F<sub>4</sub>TCNQ dimer and the anthraquinone derivate based on density functional theory (DFT) calculations. The structures of the investigated molecules are shown in Fig. 1.

The electronic structure of the anthraquinone derivate as depicted in Fig. 2a has already been discussed in detail elsewhere.<sup>10,14</sup> It shows the typical properties of a  $\pi$ -conjugated molecular material (semiconductor) having a HOMO-LUMO gap of about 1.6 eV and an almost symmetric level arrangement. The HOMO and HOMO-1 levels are delocalized and span the whole molecule including the thiol anchor units. The sprawling side structures guarantee that the electron withdrawing or pushing effects of the anchor units only slightly modify the underlying electronic structure of the anthraquinone core.

The electronic structure of the picene-F<sub>4</sub>TCNQ system on the other hand is determined by the occurrence of hybrid orbitals which are formed between the  $\pi$ -conjugated picene and the F<sub>4</sub>TCNQ acceptor. The HOMO-1 and LUMO orbitals of picene-F<sub>4</sub>TCNQ are formed from states of the free picene and F<sub>4</sub>TCNQ. This hybridization induces a charge transfer of about  $0.2e$  from the picene to the F<sub>4</sub>TCNQ.<sup>7</sup>

Based on the electronic structure calculations the transport properties have been obtained using the non-equilibrium Green function formalism (NEGF). Both molecular systems are sandwiched between two Au(111) leads. Fig. 3 shows the  $I$ - $V$  curves without gate voltage (black lines) for the (a) anthraquinone and (b) picene-F<sub>4</sub>TCNQ system. Both curves show typical details which are expected from the  $I$ - $V$  characteristics of a molecular junction. Due to the weak coupling of both molecular systems to the Au(111) leads both systems show features which can be attributed to distinct molecular orbitals.

In a very simplified picture, if the bias voltage is rising then more orbitals will contribute to the conduction through the

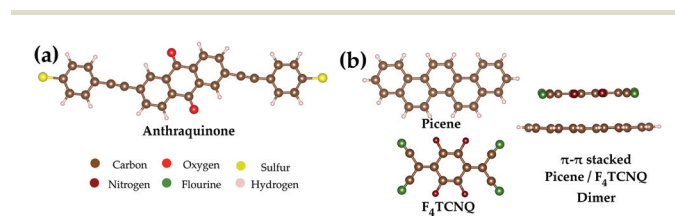


Fig. 1 Schematic drawings of the molecules as used in the electronic structure and quantum transport calculations: (a) the anthraquinone derivate and (b) the picene-F<sub>4</sub>TCNQ dimer.

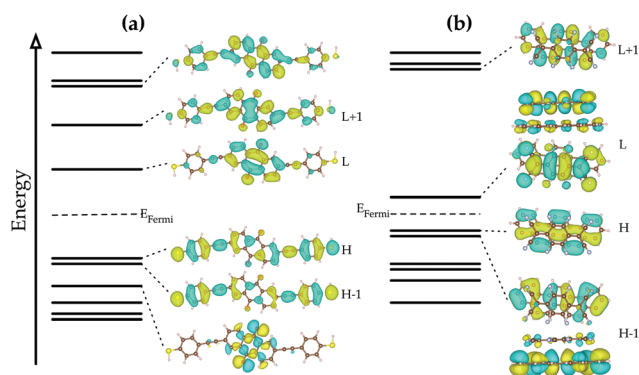


Fig. 2 Electronic structure close to the Fermi level as obtained from density functional theory calculations for (a) the anthraquinone derivate and (b) the picene-F<sub>4</sub>TCNQ dimer.

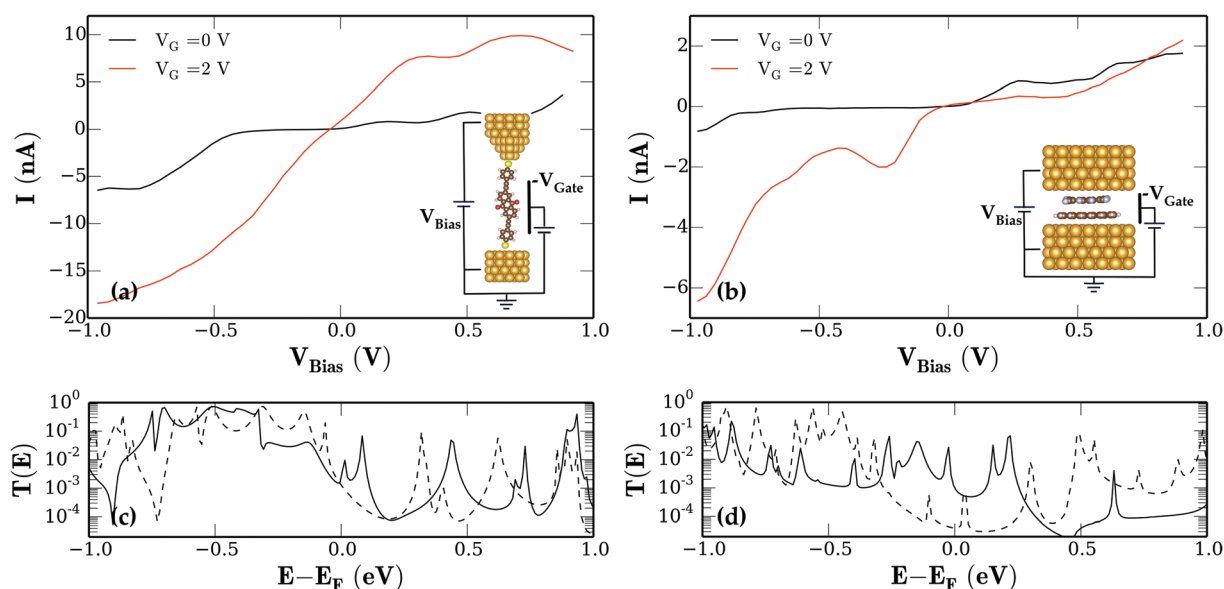


Fig. 3 Calculated transport characteristics of the anthraquinone reference system (a) and the picene-F<sub>4</sub>TCNQ model device (b). The reference system shows moderate enhancement of the current in both bias directions. In contrast the picene-F<sub>4</sub>TCNQ shows a very strong increase only in the reverse-bias region while the forward-bias current is nearly not affected by the external gate field. (c), (d) Respective transmission spectra  $T(E)$  for the molecular junctions at zero (solid line) and  $-0.75$  V (dashed line) bias.



junction and the current increases. Peaks or regions of negative differential resistance (NDR) occur if distinct levels contribute to the conduction on low bias voltages and do not contribute in the case of high bias voltages due to *e.g.* the lowering of the coupling strength between the molecular orbital and the lead.<sup>12,17</sup> Such a situation can be seen, for example, in the anthraquinone system at  $\approx 0.2$  V and  $\approx 0.5$  V bias voltages and for the picene- $F_4$ TCNQ system at  $V_{\text{bias}} \approx 0.25$  V.

The effect of increasing bias voltage on the electron transmission spectra of the two molecular junctions is depicted in Fig. 3c and d, respectively. In the zero bias transmission function the picene- $F_4$ TCNQ system (solid line) has a prominent feature at 0.2 eV above the Fermi level ( $E_F$ ) which can be attributed to the LUMO level of the dimer. The features right below  $E_F$  are therefore linked to the HOMO, HOMO-1, *etc.* dimer orbitals. Above 0.3 eV picene- $F_4$ TCNQ exhibits no features relevant to transport.

The main effects of an applied bias voltage on a molecular junction are (i) shifting the transmission spectra with respect to  $V_{\text{bias}}$ , (ii) strengthening and dampening of transmission features due to the bias induced changes in the molecule-lead coupling and (iii) widening of the energy window in which transmission peaks contribute to the current. Therefore if we apply a positive bias to the picene- $F_4$ TCNQ junction we are shifting transmission features which correspond to occupied HOMO- $n$  orbitals into the energy window relevant for conduction. For negative bias the transmission peaks originating from the HOMO and LUMO are shifted out of that window and due to the large energy gap between the LUMO and LUMO+ $n$  levels (see Fig. 2b), there are no additional levels which can contribute to the conduction. Only in the case of very high bias voltages  $>1$  V can additional transmission features appear and the current starts to rise also for negative bias.

For the anthraquinone junction the situation is completely different. We observe a somewhat lower density of transmission peaks for energies above  $E_F$  (see Fig. 3c). The changes in the bias voltage do not significantly change the overall density of transmission peaks in the energy window around  $E_F$  contributing to the conduction. Hence the absolute value of the current through the junction is approximately the same whether we apply a negative or positive bias voltage. Our results are in good agreement with other theoretical estimates.<sup>12,13</sup> In the picene- $F_4$ TCNQ junction (Fig. 3b) the current for the negative bias case stays almost at zero up to an  $V_{\text{bias}} < -0.8$  V. For the anthraquinone junction (Fig. 3a) the current rises more or less symmetrically in the case of forward and reverse bias.

This asymmetric behavior gives rise to large current rectification for the picene- $F_4$ TCNQ system. The rectification ratio can be defined as  $R(V) = |I(V)/I(-V)|$ .<sup>6</sup> We show a comparison of  $R$  for the two systems in the voltage range of interest in Fig. 4b. The highest  $R$  are achievable for very low values of  $V$ ; however, for real applications voltages between 0.2 and 0.8 V seem to be more manageable whereas higher bias voltages may lead to rapid degradation in the organic material.<sup>18</sup> From our calculation we obtain rectification ratios for  $R_{\text{Picene}} \approx 20$ , which is much higher than the achievable maximum values for  $R_{\text{AQ}}$ . Moreover for the anthraquinone system we find a steep decrease of the rectification up to  $\approx 0.6$  V whereas the picene- $F_4$ TCNQ system shows only a weak dependence in the considered bias range.

For further analysis of the rectifying mechanism we calculated the charge transfer of the picene- $F_4$ TCNQ dimer as a function of the applied bias voltage (see ESI S2†). The amount of transferred charge between the molecular subunits clearly depends on the applied bias voltage. Therefore one possibility

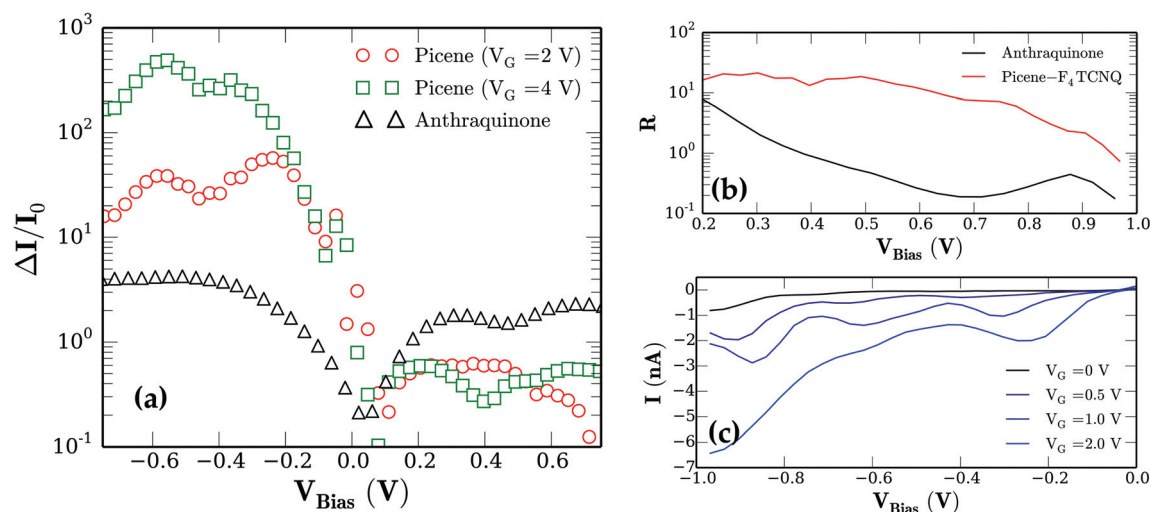


**Fig. 4** (a) Current across the picene- $F_4$ TCNQ model junction compared to the anthraquinone reference system as a function of the bias voltage at different gate voltages ( $I_0$  is the respective current without gate voltage). (b) Rectification ratio  $R(V) = |I(V)/I(-V)|$  for the two molecular junctions under investigation. (c) Calculated change in the reverse bias current across the picene- $F_4$ TCNQ model junction as a function of the applied gate voltage  $V_G$ .



of rationalizing the working principle of the picene/ $F_4$ TCNQ system as a molecular diode is to see the system as a natural pn-junction due to the charge transfer creating the anode and cathode side of the molecular stack. The weak rectifying characteristic of the anthraquinone system on the other hand mainly originate from small differences in the coupling of the molecule to the electrodes in combination with moderate evolution of transmission features under applied bias. It is also important with note that compared to the original model of a molecular diode proposed by Aviram and Ratner,<sup>1</sup> we observe a reversed rectification direction. However, this is in qualitative agreement with the results reported on different molecular systems.<sup>19,20</sup> In the original model, the rectification mechanism is due to the difference in the tunneling rates between the donor and acceptor part of the molecular structure. In contrast to the DFT-NEGF method used for the present calculations the original model also considered only the HOMO and LUMO molecular orbitals and neglected any bias-induced changes of the electronic structure as well as changes in the molecule-electrode coupling. Hence the potential barrier built by the charge transfer inside the picene- $F_4$ TCNQ dimer in combination with the large asymmetry of the molecular transmission features are clearly the reasons for the observed direction and height of the rectification effect.

With its large rectification values the picene- $F_4$ TCNQ system also outweighs already reported maximum values for other charge transfer and molecular materials by at least one order of magnitude.<sup>4,6</sup> The low variability of  $R_{\text{picene}}$  over a wide bias range seems more appropriate for real world applications. In consequence we propose the picene- $F_4$ TCNQ system as a molecular material to fabricate organic diodes due to its advantageous forward and reverse bias properties.

Further, a required key element for implementing real molecular circuits is electrical switching. For that reason we compared the response of the two molecular systems to the application of an external gate voltage  $V_{\text{Gate}}$  as schematically shown in the insets of Fig. 3. Therefore an additional uniform electric field applied as an external potential was used to model the gate electrode. The  $I$ - $V$  curves corresponding to a  $V_{\text{Gate}} = 2$  V for the respective junctions are also shown as red lines in Fig. 3a and b. Both systems show a rather strong response to the application of an external gate field. For better quantification of the effect, the change of the current due to the applied gate voltage  $\Delta I = |I_0 - I_{\text{Gate}}|$  normalized to current without gate  $I_0$  for both systems is presented in Fig. 4a.

For the anthraquinone junction we find a constant increase of the current for  $|V_{\text{bias}}| > 0.2$  V between a factor of two and three. Other authors report very large on/off ratios for anthraquinone junctions of  $>1 \times 10^3$ . However, these ratios are achieved by chemical modification of the molecule itself and are potentially irreversible in contrast to the electrical switching presented here. Additionally the already mentioned theoretical<sup>12-15</sup> as well as recently measured data<sup>14</sup> on anthraquinone systems all show almost symmetrical behavior of the  $I$ - $V$  characteristics. The additional gate field in the junction induces two main effects. First the gate voltage shifts the mole-

cular energy levels with respect to the energy window in which molecular orbitals contribute to the conduction (see ref. 21). In the present case the positive gate voltage results in a higher number of occupied molecular levels contributing and hence the current increases. The second effect of the gate field is the induction of changes of the electronic structure of the molecule itself. DFT calculations on the anthraquinone molecule with an applied electric field equal to the gate field in the transport calculations indicate that for example the HOMO-LUMO gap of the molecule is reduced and the molecular level alignment changes as well. In Fig. 4a one can see that the amplification of the current due to the gate field for the anthraquinone junction is almost symmetrical with respect to the bias voltage.

The same effects of a gate field also occur in the case of the picene junction. However, due to the asymmetric character of the molecular orbitals around the Fermi level the impact on the  $I$ - $V$  characteristics is much larger. Under forward bias the current is barely affected by the gate voltage. In fact the current even shows a small decrease. For the reverse bias case, however, we see a large increase of the current due to gate voltage. We achieve a maximum switching effect by about  $5 \times 10^2$  for a gate voltage  $V_G = 4$  V (see Fig. 4a). In Fig. 4c we additionally show in more detail the dependence of the reverse bias current of the picene- $F_4$ TCNQ junction as a function of the applied gate voltage.

As mentioned before the large energy distance between the LUMO and LUMO+1 leads to almost no transmission for reverse bias. As the gate field shifts the molecular levels we see of course a current increase. However, this level shifting alone does not explain the quantity of the observed effect. Here a further mechanism comes into play for the picene- $F_4$ TCNQ system. As discussed in the beginning the picene- $F_4$ TCNQ is a weakly bonded dimer with charge transfer of  $\approx 0.2$  electrons from the picene to  $F_4$ TCNQ. Our DFT calculations on the picene- $F_4$ TCNQ dimer with an electric field applied perpendicular to the stacking direction (= transport direction) reveal that the hybridization of the dimer itself depends strongly on the applied field. The applied electric field allows us to tune the hybridization between the dimer components. This allows us to lower the LUMO-LUMO+ $n$  distance drastically. The result is that in the reverse bias case with the gate field switched on, the number of levels which account to the conduction is increased. This explains the very large switching ratios of  $5 \times 10^2$ .

In addition we wish to point out that this behavior corresponds perfectly to the arguments given by Ratner and coworkers<sup>1,2</sup> for achieving molecular rectification. Local weak links in a molecule, given in our case through the hybridization in the picene- $F_4$ TCNQ dimer, can result in large rectification ratios whereas strong bonding suppresses the effect. By direct modification of the hybrid levels using a gate field one can reach effective current switching. We believe that this mechanism is quite general for charge transfer systems and should be applicable to other dimer systems as well.<sup>22</sup>





### 3. Summary

To summarize, the NEGF + DFT studies of the anthraquinone–Au(111) and picene–F<sub>4</sub>TCNQ–Au(111) systems have shown that the respective systems exhibit fundamentally different *I*–*V* characteristics. The anthraquinone system shows an approximately ohmic behavior for low bias voltages and the application of an external gate field results in an increase of the overall current through the junction which is almost symmetric for positive and negative bias voltages.

Due to hybrid dimer states close to the Fermi level the picene–F<sub>4</sub>TCNQ *I*–*V* curve is very asymmetric, with a pronounced diode-like forward/reverse current behavior. In contrast to the anthraquinone system the effect of an applied gate voltage is about two orders of magnitude larger in the reverse bias than in the forward bias case.

Further, we have shown that the anthraquinone system can also be seen as an electrically controllable switch. However, in terms of achieving maximum switching ratios the picene–F<sub>4</sub>TCNQ junction shows a clear benefit and can be seen as a molecular transistor in terms of classical circuit elements. The anthraquinone system on the other hand offers almost symmetric and linear *I*–*V* characteristics in the  $V_{\text{bias}} \pm 0.3$  V range and may be better utilized as an operational amplifier.

Consequently, we propose to use the pure organic interface between picene and F<sub>4</sub>TCNQ as a straightforward way to manufacture a molecular switch with a very large switching ratio or a molecular transistor/amplifier. It should be kept in mind that the presented results rely on the systematic limitations of the applied theoretical model. Many-body and strong correlation effects, in particular, are not included. Nevertheless, for the presented cases of low bias voltages the forecasts of the DFT/NEGF method are known to be qualitatively correct.

### 4. Methods

The ground state electronic structure of the molecules was investigated using the all-electron density functional theory (DFT) NRLMOL program package which achieves a high level of numerical accuracy (see ref. 23, 24 and references therein). For the exchange correlation GGA/PBE<sup>25</sup> was used, and in all calculations the dispersion correction utilizing the DFT-D2 method<sup>26</sup> was included. The geometry of the molecules was optimized using a gradient approach; the relaxation was terminated once all atomic forces were below 0.05 eV Å<sup>−1</sup>. We applied the nonequilibrium Green's function method (NEGF) for self-consistent calculation of the electron transport properties as implemented in the GPAW code<sup>27,28</sup> to investigate the *I*–*V* characteristics of our model devices. For the transport calculations the electronic structure is obtained by DFT calculations using the common approach of constructing a model device where the molecule of interest together with additional electrode atoms (scattering region) are sandwiched between two semi-infinite (metallic) electrodes. In our case we used at least three additional Au(111) layers on each side of

the molecule to construct the scattering region followed by a further geometry optimization step of the system where the topmost two gold layers together with the attached molecules were allowed to relax. For the scattering region as well as for the leads a localized double- $\zeta$  polarized basis set was used. Schematic drawings of the used model junctions are shown in the insets in Fig. 3. The whole system can be subjected to an external bias and/or gate voltage. The electronic structure of the scattering region and therefore the *I*–*V* curves are calculated self-consistently in the presence of such external fields. To support the deductions in this paper we merely repeat the key facts of the DFT-NEGF method of use whilst a detailed discussion of the method can be found in the cited literature. The GPAW transport code uses the Green's function of the central region defined by

$$G(E) = [ES - H_C - \sum_L (E) - \sum_R (E)]^{-1} \quad (1)$$

where *S* and *H<sub>C</sub>* are the overlap and Hamiltonian matrix of the scattering region written in the localized basis.  $\sum_{L/R}$  are the

respective self energies of the leads. After self-consistency in the cycle  $G \rightarrow n(r) \rightarrow v(r) \rightarrow H_C \rightarrow G$  is reached the transmission function is calculated by

$$T(E, V) = \text{Tr}[G(E)\Gamma_L(E)G(E)^\dagger\Gamma_R(E)] \quad (2)$$

with  $\Gamma_{L/R}(E) = i\left(\sum_{L/R}(E) - \sum_{L/R}(E)^\dagger\right)$ . Therefore *T*(*E*, *V*) gives the transmission probability of an electron having an energy *E* under an applied bias (and gate) voltage *V*. Further, the current through the junction is obtained by

$$I(V) = \frac{2e^2}{h} \int_{\mu_L}^{\mu_R} T(E, V) dE \quad (3)$$

where the electronic chemical potentials  $\mu_{L/R}$  are connected to the applied bias voltage via  $V = (\mu_L - \mu_R)/e$  (*e* elementary charge).<sup>29</sup> *De facto* the current is calculated by integrating the self-consistent transmission function within the bias-dependent energy window spanned by  $\mu_{L/R}$ .

### Acknowledgements

Financial support by the Deutsche Forschungsgemeinschaft within the Forschergruppe FOR 1154, project KO1924/5 and by the saxonian cluster of excellence "Structure Design of Novel High-Performance Materials via Atomic Design and Defect Engineering (ADDE)" is gratefully acknowledged. We especially thank the ZIH Dresden for providing extensive computational resources and support.



## References

- 1 A. Aviram and M. A. Ratner, Molecular rectifiers, *Chem. Phys. Lett.*, 1974, **29**, 277–283.
- 2 V. Mujica, M. A. Ratner and A. Nitzan, Molecular rectification: why is it so rare?, *Chem. Phys.*, 2002, **281**, 147–150.
- 3 R. M. Metzger, Unimolecular electronics, *J. Mater. Chem.*, 2008, **18**, 4364.
- 4 K.-G. Zhou, *et al.* Can azulene-like molecules function as substitution-free molecular rectifiers?, *Phys. Chem. Chem. Phys.*, 2011, **13**, 15882–15890.
- 5 S. Kubatkin, *et al.* Single-electron transistor of a single organic molecule with access to several redox states, *Nature*, 2003, **425**, 698–701.
- 6 Y. Tsuji, A. Staykov and K. Yoshizawa, Molecular Rectifier Based on Stacked Charge Transfer Complex, *J. Phys. Chem. C*, 2012, **116**, 2575–2580.
- 7 B. Mahns, *et al.* Crystal Growth, Structure, and Transport Properties of the Charge-Transfer Salt Picene/2,3,5,6-Tetrafluoro-7,7,8,8-tetracyanoquinodimethane, *Cryst. Growth Des.*, 2014, **14**, 1338–1346.
- 8 E. H. van Dijk, D. J. T. Myles, M. H. van der Veen and J. C. Hummelen, Synthesis and properties of an anthraquinone-based redox switch for molecular electronics, *Org. Lett.*, 2006, **8**, 2333–2336.
- 9 T. Markussen, J. Schitz and K. S. Thygesen, Electrochemical control of quantum interference in anthraquinone-based molecular switches, *J. Chem. Phys.*, 2010, **132**, 224104.
- 10 N. Seidel, *et al.* Synthesis and properties of new 9,10-anthraquinone derived compounds for molecular electronics, *New J. Chem.*, 2013, **37**, 601.
- 11 A. Batra, *et al.* Tuning rectification in single-molecular diodes, *Nano Lett.*, 2013, **13**, 6233–6237.
- 12 P. Zhao and D.-S. Liu, Electronic Transport Properties of an anthraquinone-Based Molecular Switch with Carbon Nanotube Electrodes, *Chin. Phys. Lett.*, 2012, **29**, 047302.
- 13 P. Zhao, *et al.* First-principles study of the electronic transport properties of the anthraquinone-based molecular switch, *Phys. Rev. B: Condens. Matter*, 2011, **406**, 895–898.
- 14 C. M. Gudon, *et al.* Observation of quantum interference in molecular charge transport, *Nat. Nanotechnol.*, 2012, **7**, 305–309.
- 15 H. Valkenier, *et al.* Cross-conjugation and quantum interference: a general correlation?, *Phys. Chem. Chem. Phys.*, 2014, **16**, 653–662.
- 16 N. Darwish, *et al.* Single Molecular Switches: Electrochemical Gating of a Single Anthraquinone-Based Norbornylogous Bridge Molecule, *J. Phys. Chem. C*, 2012, **116**, 21093–21097.
- 17 S. Karthuser, Control of molecule-based transport for future molecular devices, *J. Phys. Condens. Matter*, 2011, **23**, 013001.
- 18 G. Schulze, *et al.* Resonant Electron Heating and Molecular Phonon Cooling in Single C60 Junctions, *Phys. Rev. Lett.*, 2008, **100**, 136801.
- 19 J. B. Pan, Z. H. Zhang, X. Q. Deng, M. Qiu and C. Guo, Rectifying performance of D- $\pi$ -A molecules based on cyano-vinyl aniline derivatives, *Appl. Phys. Lett.*, 2010, **97**, 203104.
- 20 J. Taylor, M. Brandbyge and K. Stokbro, Theory of Rectification in Tour Wires: The Role of Electrode Coupling, *Phys. Rev. Lett.*, 2002, **89**, 138301.
- 21 L. Bogani and W. Wernsdorfer, Molecular spintronics using single-molecule magnets, *Nat. Mater.*, 2008, **7**, 179–186.
- 22 S. Lindner, M. Knupfer, R. Friedrich, T. Hahn and J. Kortus, Hybrid States and Charge Transfer at a Phthalocyanine Heterojunction: MnPc/F16CoPc, *Phys. Rev. Lett.*, 2012, **109**, 027601.
- 23 M. R. Pederson, D. V. Porezag, J. Kortus and D. C. Patton, Strategies for Massively Parallel Local-Orbital-Based Electronic Structure Methods, *Phys. Status Solidi*, 2000, **217**, 197–218.
- 24 D. Porezag and M. Pederson, Optimization of Gaussian basis sets for density-functional calculations, *Phys. Rev. A*, 1999, **60**, 2840–2847.
- 25 J. P. Perdew, K. Burke and M. Ernzerhof, Generalized Gradient Approximation Made Simple, *Phys. Rev. Lett.*, 1996, **77**, 3865–3868.
- 26 S. Grimme, Semiempirical GGA-type density functional constructed with a long-range dispersion correction, *J. Comput. Chem.*, 2006, **27**, 1787–1799.
- 27 J. Chen, K. S. Thygesen and K. W. Jacobsen, Ab initio nonequilibrium quantum transport and forces with the real-space projector augmented wave method, *Phys. Rev. B: Condens. Matter*, 2012, **85**, 155140.
- 28 J. Enkovaara, *et al.* Electronic structure calculations with GPAW: a real-space implementation of the projector augmented-wave method, *J. Phys. Condens. Matter*, 2010, **22**, 253202.
- 29 Y. Meir and N. Wingreen, Landauer formula for the current through an interacting electron region, *Phys. Rev. Lett.*, 1992, **68**, 2512–2515.

